



# Searches for 28 rare and forbidden decays of $D^+$ and $D^+_s$ mesons.

IOP Conference

04-April-22

**Zakariya Aliouche,**

Chris Parkes, Chris Burr, Fergus Wilson, Raja Nandakumar

# Motivations - Rare and forbidden decays

Rare and forbidden decays are an important tool in the search for BSM (Beyond Standard Model) physics.

Rare decays are heavily suppressed in the SM, and can be used as an important test of the SM's characterisation of such decays. This analysis will consider rare decays that occur via Weak annihilation or FCNC (Flavour Changing Neutral Current) transitions.

In SM, only Weak annihilation occurs at tree level and can be singly or doubly Cabibbo Favoured /Supressed (CF/CS) depending on the quark transitions. FCNC transitions exist at the loop level and are suppressed via the GIM mechanism (Glashow—Iliopoulos—Maian) [DOI:<https://doi.org/10.1103/PhysRevD.2.1285>].

LHCb has seen anomalies in Lepton Universality measurements in B decays [<https://doi.org/10.1038/nature14474>] which could be an indicator of BSM physics involving leptons. Observing decays forbidden in the SM by Lepton Number or Flavour Violation (LNV/LFV) would all be indications of BSM Physics.

# Motivations - $D_{(s)}^+ \rightarrow h^\pm l^\mp l^{(\prime)+}$

Searches are performed for rare or forbidden charm decays using decay channels of the form  $D_{(s)}^+ \rightarrow h^\pm l^\mp l^{(\prime)+}$ , where  $h^\pm$  is a  $\pi$  or  $K$  and  $l^\pm$  is an  $e$  or  $\mu$ .

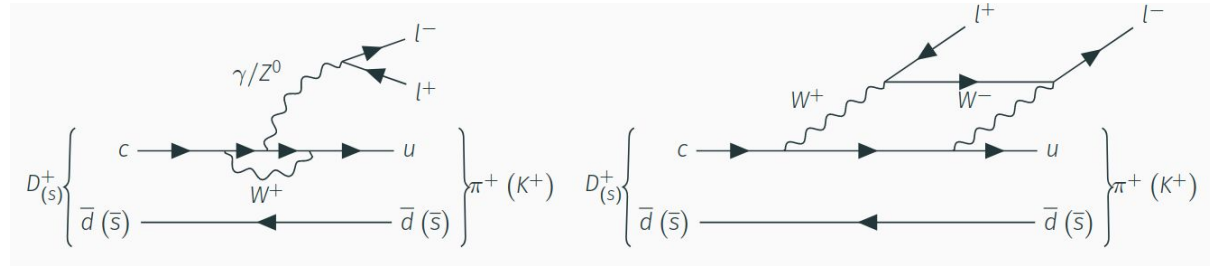
There are 28 decay modes considered. The physics interest of these channels varies: the commonality is in the experimental procedures.

The 8 decays highlighted in green are allowed via the SM due to Lepton Flavour or Number conservation. These occur via FCNC (Flavour Changing Neutral Current) or weak annihilation.

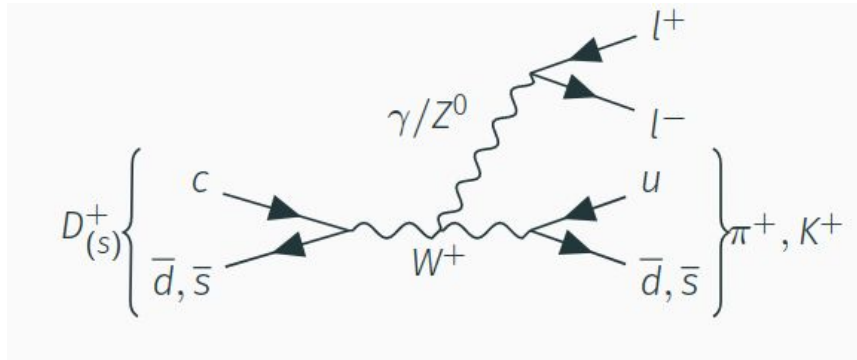
$D^+ \rightarrow K^+ \mu^+ \mu^-$	$D^+ \rightarrow \pi^+ \mu^+ \mu^-$	$D_s^+ \rightarrow K^+ \mu^+ \mu^-$	$D_s^+ \rightarrow \pi^+ \mu^+ \mu^-$
$D^+ \rightarrow K^- \mu^+ \mu^+$	$D^+ \rightarrow \pi^- \mu^+ \mu^+$	$D_s^+ \rightarrow K^- \mu^+ \mu^+$	$D_s^+ \rightarrow \pi^- \mu^+ \mu^+$
$D^+ \rightarrow K^+ \mu^+ e^-$	$D^+ \rightarrow \pi^+ \mu^+ e^-$	$D_s^+ \rightarrow K^+ \mu^+ e^-$	$D_s^+ \rightarrow \pi^+ \mu^+ e^-$
$D^+ \rightarrow K^- \mu^+ e^+$	$D^+ \rightarrow \pi^- \mu^+ e^+$	$D_s^+ \rightarrow K^- \mu^+ e^+$	$D_s^+ \rightarrow \pi^- \mu^+ e^+$
$D^+ \rightarrow K^+ e^+ \mu^-$	$D^+ \rightarrow \pi^+ e^+ \mu^-$	$D_s^+ \rightarrow K^+ e^+ \mu^-$	$D_s^+ \rightarrow \pi^+ e^+ \mu^-$
$D^+ \rightarrow K^+ e^+ e^-$	$D^+ \rightarrow \pi^+ e^+ e^-$	$D_s^+ \rightarrow K^+ e^+ e^-$	$D_s^+ \rightarrow \pi^+ e^+ e^-$
$D^+ \rightarrow K^- e^+ e^+$	$D^+ \rightarrow \pi^- e^+ e^+$	$D_s^+ \rightarrow K^- e^+ e^+$	$D_s^+ \rightarrow \pi^- e^+ e^+$

The rest of the decays are forbidden via LFV or LFV and LNV.

# Motivations- Rare SM allowed decays



Feynman diagrams for FCNC decays of a  $D_{(s)}^+$  meson



Feynman diagram of Weak annihilation decay of a  $D_{(s)}^+$  meson

Could also show LFV if non-SM couplings occur at the lepton vertices!

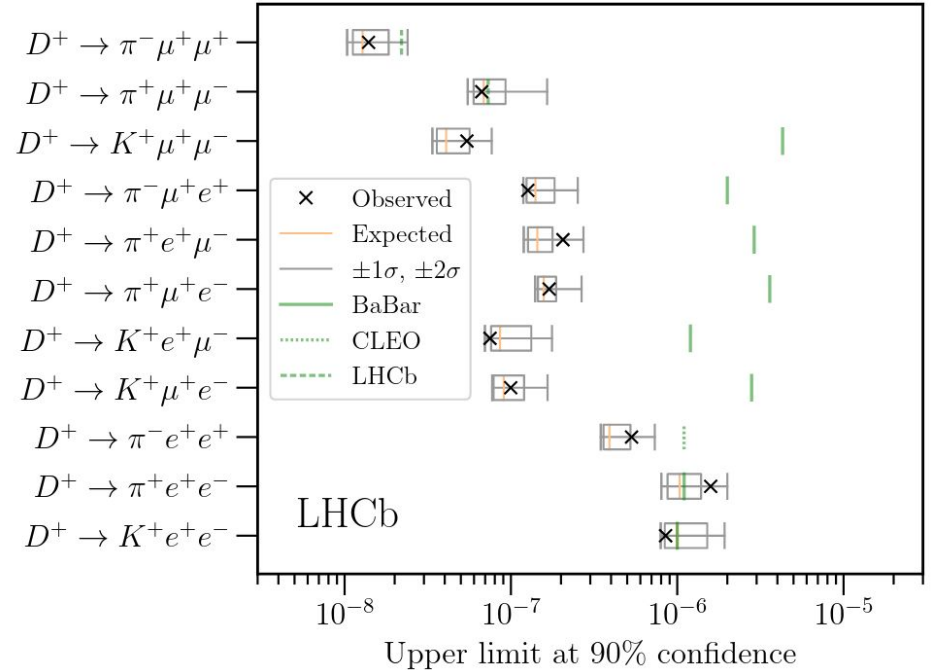
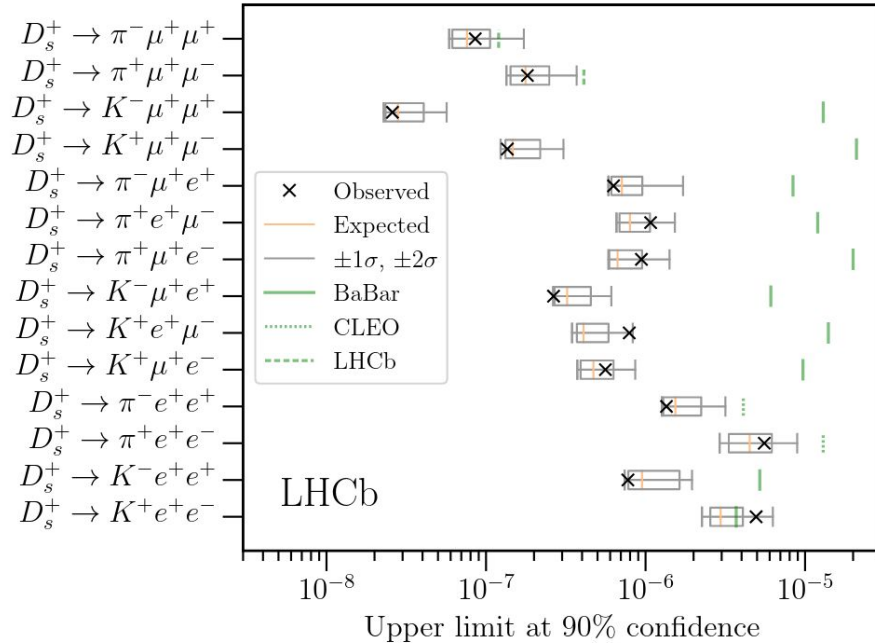
# Pathfinding analysis on 2016 data by LHCb

- Analysis procedure based off the work published on 2016 data.
- Paper “Searches for 25 rare and forbidden decays of  $D^+$  and  $D_s^+$  mesons”.  
[[https://doi.org/10.1007/JHEP06\(2021\)044](https://doi.org/10.1007/JHEP06(2021)044)]
- This analysis was done using  $1.6 \text{ fb}^{-1}$  of data from the 2016 run.

Channel	Type	Current Limit	Experiment	Resonance	Channel	Type	Current Limit	Experiment	Resonance
$D^+ \rightarrow \pi^+ e^+ e^-$	FCNC	$< 1.1 \times 10^{-6}$	BABAR [1]	$\phi, 1.7 \times 10^{-6}$	$D_s^+ \rightarrow \pi^+ e^+ e^-$	Weak annihilation CF	$< 13 \times 10^{-6}$	CLEO [3]	$\phi, 6 \times 10^{-6}$
$D^+ \rightarrow \pi^+ \mu^+ \mu^-$	FCNC	$< 7.3 \times 10^{-8}$	LHCb [2]	$\phi, 1.8 \times 10^{-6}$	$D_s^+ \rightarrow \pi^+ \mu^+ \mu^-$	Weak annihilation CF	$< 4.1 \times 10^{-7}$	LHCb [2]	Not seen
$D^+ \rightarrow K^+ e^+ e^-$	Weak annihilation DCS	$< 1.0 \times 10^{-6}$	BABAR [1]	Not Seen	$D_s^+ \rightarrow K^+ e^+ e^-$	FCNC	$< 3.7 \times 10^{-6}$	BABAR [1]	Not seen
$D^+ \rightarrow K^+ \mu^+ \mu^-$	Weak annihilation DCS	$< 4.3 \times 10^{-6}$	BABAR [1]	Not Seen	$D_s^+ \rightarrow K^+ \mu^+ \mu^-$	FCNC	$< 21 \times 10^{-6}$	BABAR [1]	Not seen
$D^+ \rightarrow \pi^+ e^+ \mu^-$	LFV	$< 2.9 \times 10^{-6}$	BABAR [1]	-	$D_s^+ \rightarrow \pi^+ e^+ \mu^-$	LFV	$< 12 \times 10^{-6}$	BABAR [1]	-
$D^+ \rightarrow \pi^+ e^- \mu^+$	LFV	$< 3.6 \times 10^{-6}$	BABAR [1]	-	$D_s^+ \rightarrow \pi^+ e^- \mu^+$	LFV	$< 20 \times 10^{-6}$	BABAR [1]	-
$D^+ \rightarrow K^+ e^+ \mu^-$	LFV	$< 1.2 \times 10^{-6}$	BABAR [1]	-	$D_s^+ \rightarrow K^+ e^+ \mu^-$	LFV	$< 14 \times 10^{-6}$	BABAR [1]	-
$D^+ \rightarrow K^+ e^- \mu^+$	LFV	$< 2.8 \times 10^{-6}$	BABAR [1]	-	$D_s^+ \rightarrow K^+ e^- \mu^+$	LFV	$< 9.7 \times 10^{-6}$	BABAR [1]	-
$D^+ \rightarrow \pi^- e^+ e^+$	LNV LFV	$< 1.1 \times 10^{-6}$	CLEO [3]	-	$D_s^+ \rightarrow \pi^- e^+ e^+$	LNV LFV	$< 4.1 \times 10^{-6}$	CLEO [3]	-
$D^+ \rightarrow \pi^- \mu^+ \mu^+$	LNV LFV	$< 2.2 \times 10^{-8}$	LHCb [2]	-	$D_s^+ \rightarrow \pi^- \mu^+ \mu^+$	LNV LFV	$< 1.2 \times 10^{-7}$	LHCb [2]	-
$D^+ \rightarrow K^- e^+ e^+$	LNV LFV	$< 0.9 \times 10^{-6}$	BABAR [1]	-	$D_s^+ \rightarrow K^- e^+ e^+$	LNV LFV	$< 5.2 \times 10^{-6}$	BABAR [1]	-
$D^+ \rightarrow K^- \mu^+ \mu^+$	LNV LFV	$< 10 \times 10^{-6}$	BABAR [1]	-	$D_s^+ \rightarrow K^- \mu^+ \mu^+$	LNV LFV	$< 1.3 \times 10^{-5}$	BABAR [1]	-
$D^+ \rightarrow \pi^- e^+ \mu^+$	LNV LFV	$< 2.0 \times 10^{-6}$	BABAR [1]	-	$D_s^+ \rightarrow \pi^- e^+ \mu^+$	LNV LFV	$< 8.4 \times 10^{-6}$	BABAR [1]	-
$D^+ \rightarrow K^- e^+ \mu^+$	LNV LFV	$< 1.9 \times 10^{-6}$	BABAR [1]	-	$D_s^+ \rightarrow K^- e^+ \mu^+$	LNV LFV	$< 6.1 \times 10^{-6}$	BABAR [1]	-

Old 90% confidence limits on the Branching ratio that the 2016 analysis improved upon (see next slide). Table nicely shows the physics interest of each decay specifically.

# Results of 2016 analysis by LHCb



The 90% CL on the branching fraction vary from  $(1.4-640) \times 10^{-8}$  [[https://doi.org/10.1007/JHEP06\(2021\)044](https://doi.org/10.1007/JHEP06(2021)044)]

# Improvements on 2016 analysis

Hope to recreate this analysis with the following improvements:

- Include 2017 and 2018 datasets (additional  $7.4 \text{ fb}^{-1}$  of data). This dataset is not identical in the way it was recorded to the 2016 dataset.
- Include 3 decay channels ( $D^+ \rightarrow K^- e^+ e^+$ ,  $D^+ \rightarrow K^- \mu^+ e^+$ ,  $D^+ \rightarrow K^- \mu^+ \mu^+$ ) that were excluded from original paper due to imperfect background characterisation.
- Improve analysis performance via normalisation channel fitting, classifier performance and PID systematics.
- Regarding the channels that contain main resonances, want to split limits to before and after the resonance by performing separate fits in the appropriate mass regions.

And to do so, here are the different channels we need to look at:

Blinded Data:

- Signal channels blinded around the  $D^+_{(s)}$  masses for blinded analysis.
- Background channels: Other decay channels of  $D^+_{(s)}$  mesons where final state particles have been missed or misidentified.
- Normalisation: The yield of the signal are normalised to the 4 decays that contain a phi resonance.

# Calculation of Branching Ratio

$$\mathcal{B}_{D_{(s)}^+ \rightarrow h^\pm \ell^+ \ell'^{\mp}} = \frac{N_{D_{(s)}^+ \rightarrow h^\pm \ell^+ \ell'^{\mp}}}{N_{D_{(s)}^+ \rightarrow (\phi \rightarrow \mu^+ \mu^-) \pi^+}} \cdot \frac{\epsilon_{D_{(s)}^+ \rightarrow (\phi \rightarrow \mu^+ \mu^-) \pi^+}}{\epsilon_{D_{(s)}^+ \rightarrow h^\pm \ell^+ \ell'^{\mp}}} \cdot \mathcal{B}_{D_{(s)}^+ \rightarrow (\phi \rightarrow \mu^+ \mu^-) \pi^+}$$

Ratio of number of events of the signal channel to control channel. The control channels are the 4 decays that contain a phi resonance:



Relative efficiency of signal channel to control channel. This is calculated from **simulation** and factorised as below. The efficiency ratio between muons and electrons is not well described in simulation, and is corrected for using ratios of control channels.

Branching ratio of control Channel.

$$\epsilon = \epsilon_{Acceptance} \cdot \epsilon_{Reconstruction} \cdot \epsilon_{Trigger} \cdot \epsilon_{Selection} \cdot \epsilon_{Tracking} \cdot (\epsilon_{Electron})$$

# Selection of data

The data goes through a large amount of selection that is unchanged from the previous analysis

[\[https://doi.org/10.1007/IHEP06\(2021\)044\]](https://doi.org/10.1007/IHEP06(2021)044):

**L0 (Hardware Trigger):** Selection made based off hardware observables such as deposits of high Pt in hadronic calorimeter. Depending on the final state leptons, this is supplemented by selection of events with high transverse-energy clusters in the electromagnetic calorimeter and high transverse-momentum muon

**HLT1 and HLT2 (Software Triggers)** applied, with some notable physics interest in HLT2 selections of:

- **$\chi^2$  track**  $< 3$  (Normalised  $\chi^2$  that represents probability of track fit.)
- **DOC<sub>Amin</sub>**  $< 0.1$  (Cut on maximum distance of closest approach between all possible pairs of particles)
- **PT**  $> 300\text{MeV}$  (Cut on transverse momentum)
- **BPVVDCHI2**  $> 20.0$  (Cut on  $\chi^2$  distance to the related Primary Vertex (PV) )
- **P**  $> 3000\text{MeV}$  (Cut on total momentum cut)
- **ALLSAMEBPV** (Requires all particles come from the same PV)

These are applied to all 3 tracks where appropriate and there is similarly a cut on reconstructed mass candidates after fitting them to a vertex.

PID criteria are also applied to the tracks and we use an MVA to discriminate between signal and background events.

# Reweighting of Data and Simulation

- Agreement between real and simulated data is imperfect, therefore it is important to reweight them as the results of the analysis depends directly on the relative efficiencies of the particular signal channel to  $D^+_{(s)} \rightarrow (\phi \rightarrow \mu^- \mu^+) \pi^+$  being the same in data and MC.
- Reweighting is done by using a gradient boosted ensemble of decision trees and training them to distinguish between real and simulated data. The results are used to generate weights that can negate the difference.

# Fitting

Signal fitting is the one dimensional fit to the invariant mass of the  $D^+_{(s)}$  and is used to obtain a signal yield for each decay.

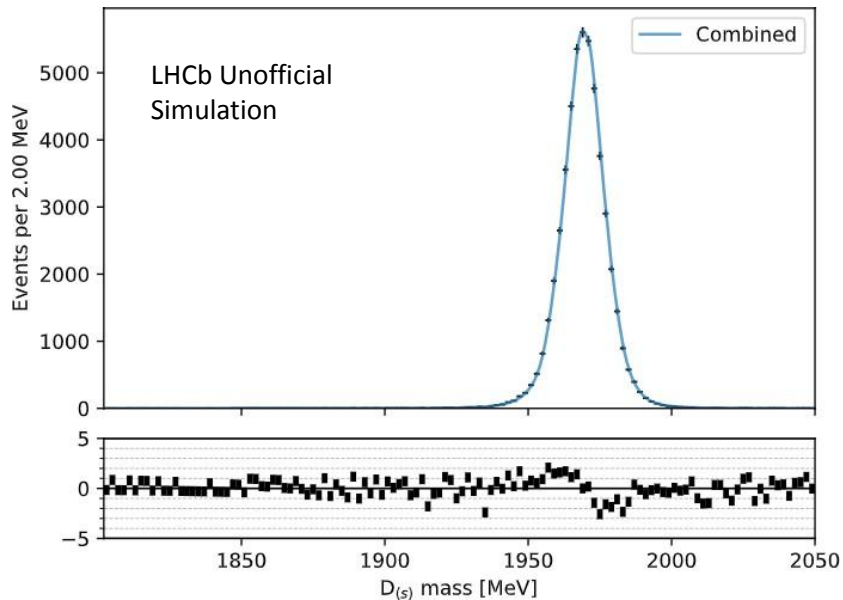
Signal prefits from simulation are used to extract signal shapes, done via the Kernel Density Estimation method (KDE) to phase space MC:

- Dimuon channels – Triple Gaussian.
- Electron without Bremsstrahlung – Crystal Ball.
- Electron with Bremsstrahlung – Asymmetric Gaussian with polynomial tails.
  - One shape per electron number.

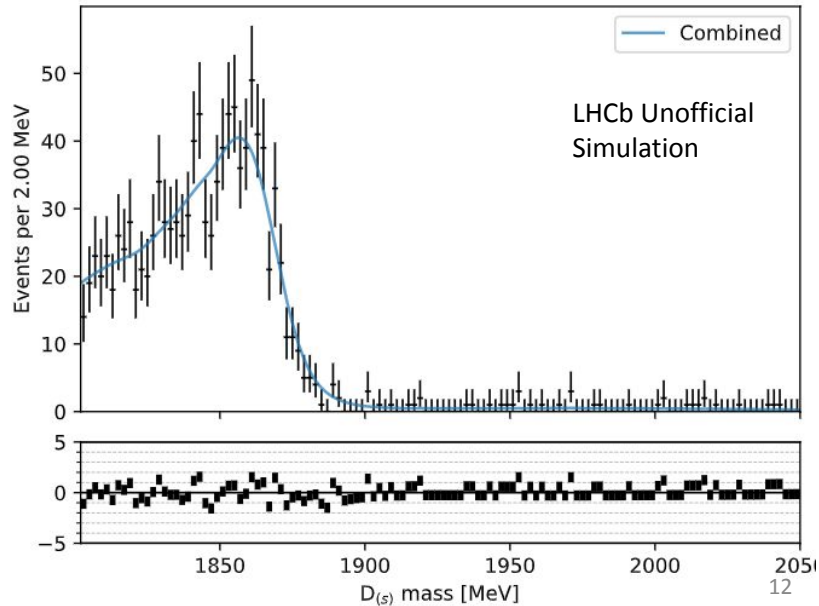
# Fitting - Simulation Prefits

- Examples of first signal pre-fit plots from simulation.
- The “Combined” line is a kernel density estimation of the simulated data.

2018 -  $D_s^+ \rightarrow K^+ \mu^- \mu^+$

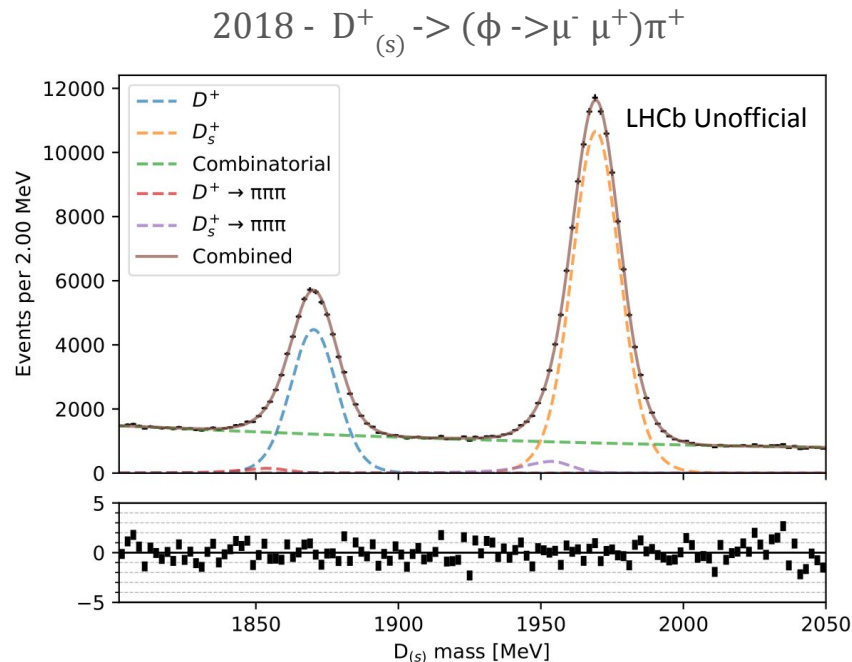
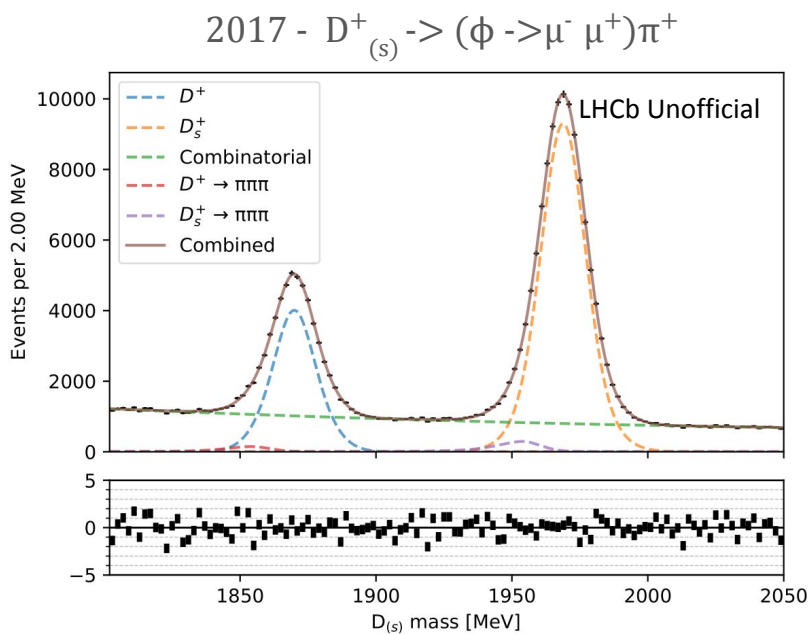


2018 -  $D^+ \rightarrow K^+ e^- e^+$



# Analysis Steps – Fitting of Normalisation Channels

Fitted normalisation channel  $D^+_{(s)} \rightarrow (\phi \rightarrow \mu^- \mu^+) \pi^+$  using 2017 and 2018 data plotted on the left and right respectively.



# Conclusion

With the increased dataset we naively expect approximately a factor 4 improvement on 90% CL on the Branching ratio: from  $(1.4-640) \times 10^{-8} \sim > (0.4-160) \times 10^{-8}$ .

Next steps:

- Optimise signal to background rejection using MVA for the 2017 and 2018 data.
- Improve PID systematics
- Include 3 missed channels from 2016 paper ( $D^+ \rightarrow K^- e^+ e^+$ ,  $D^+ \rightarrow K^- \mu^+ e^+$ ,  $D^+ \rightarrow K^- \mu^+ \mu^+$ )
- Perform fits to 28 modes and extract branching fractions and limits.

Hope this analysis will contribute to the HFLAV plots and generate interest in Rare and forbidden decays in the charm sector with exciting results and implications!

Thank you for listening!